Molecular Mass Determination of Saturated Hydrocarbons: Reactivity of η^5-Cyclopentadienylcobalt Ion (CpCo$^{\bullet+}$) and Linear Alkanes up to C-30

H. C. Michelle Byrd* and Charles M. Guttman
National Institute of Standards and Technology, Polymers Division, Gaithersburg, Maryland, USA

Douglas P. Ridge
Department of Chemistry and Biochemistry, University of Delaware, Newark, Delaware, USA

The present study demonstrates the feasibility of the η^5-cyclopentadienylcobalt ion (CpCo$^{\bullet+}$) as a suitable cationization reagent for saturated hydrocarbon analysis by mass spectrometry. Ion/molecule reactions of CpCo$^{\bullet+}$ and three medium chain-length n-alkanes were examined using Fourier-transform ion cyclotron resonance mass spectrometry. Second-order rate constants and reaction efficiencies were determined for the reactions studied. Loss of two hydrogen molecules from the CpCo-alkane ion complex was found to dominate all reactions ($\geq$80%). Furthermore, this dehydrogenation reaction efficiency increases with increasing chain length. These preliminary results suggest that the CpCo$^{\bullet+}$ ion may be a promising cationization reagent of longer chain saturated hydrocarbons and polyolefins. (J Am Soc Mass Spectrom 2003, 14, 51–57) © 2003 American Society for Mass Spectrometry

Saturated hydrocarbon polymers, polyethylene, polypropylene, and their derivatives, are the most widely used of all synthetic polymers. Their molecular structure, chemical composition, and the molecular-mass distribution (MMD) are critical in determining performance properties. The potential for rapid and direct measurement of single-chain composition and MMD makes mass spectrometry (MS) especially attractive to the polymer industry [1]. However, using MS analysis for the determination of MMDs requires the formation of intact macromolecular ions in the gas phase, which has proven to be quite difficult for saturated hydrocarbon polymers (commonly referred to as polyolefins).

Polar polymers, such as polyesters, polyglycols, and polyamides, have functional groups that can be readily cationized, usually by Na$^+$ or K$^+$ ions [1–7]. Nonpolar polymers, such as polystyrenes and polybutadienes, may be cationized via interactions between their pi-electrons and transition metal ion d-orbitals, e.g., Ag$^+$ or Cu$^+$ ions [2, 4–7]. However, saturated hydrocarbon polymers lack a suitable ionizable site on the aliphatic chain and therefore require another method of ionization.

Ideally, ionization of saturated polyolefins for MMD determination requires that (1) chemical modification of the hydrocarbon occurs inside the mass spectrometer, (2) the hydrocarbon does not require the presence or addition of a functional group for ionization to occur, (3) the predominant reaction pathway leads to a product characteristic of the original hydrocarbon, and (4) minimal side reactions and chain fragmentation would occur reducing complications with accurate molecular mass determination. Currently, there are two main strategies for tackling the polyolefin ionization challenge: (1) chemical derivatization of the polyolefin and (2) "bare" (atomic) transition metal cationization in the gas phase [8–15]. Neither meet the above four criteria.
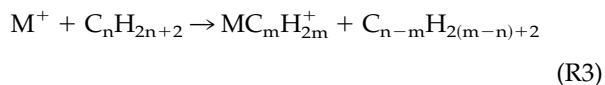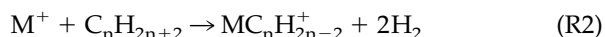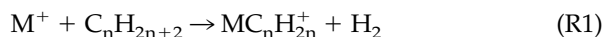
Several research groups have performed the chemical derivatization necessary for ionization by either chemically modifying the polymer to an organic salt or chemically attaching a functional group that can be readily ionized by a cation or electron attachment or deprotonation [8–12]. The main disadvantage to the chemical modification methods is that the polymer must contain a reactive end group, typically a vinyl or halide. Some but not all commercially available polyethylenes contain vinyl-terminated chains which are formed by chain transfer termination during polymerization. The reactive vinyl group is chemically modified to form the desired functionality. However, this vinyl-terminated series may not be representative of the main polymer series and may introduce a mass bias upon

chemical derivatization. Furthermore, the derivatization process requires at least two days for synthesis and purification costing time and expense.

Gas-phase studies have shown that many first-row transition metal ions react with various linear and cyclic saturated aliphatic hydrocarbons [13–17]. Fe^+, Co^+, and Ni^+ react efficiently with low molecular mass alkanes (C_nH_{2n+2}, n < 8) by dehydrogenation (Reactions 1 and 2) and dealkylation (Reaction 3) [16].

$$M^+ + C_nH_{2n+2} \rightarrow MC_nH_{2n}^+ + H_2 \qquad (R1)$$

$$M^+ + C_nH_{2n+2} \rightarrow MC_nH_{2n-2}^+ + 2H_2 \qquad (R2)$$

$$M^+ + C_nH_{2n+2} \rightarrow MC_mH_{2m}^+ + C_{n-m}H_{2(m-n)+2}$$
$$(R3)$$

These reactions have provided useful insights into the reactivity of alkane C–C and C–H bonds towards transition metals. The gas phase reactivity of alkene and alkyne C–C bonds towards transition metal atomic ions such as Fe^+ is very selective and has been proposed as a means of characterizing molecular structures, e.g., [18, 19]. Allylic C–C bonds, for example, are generally much more reactive than other C–C bonds in olefins. The reactivity of alkane C–C bonds towards Fe^+ is not very selective, however. Typically in Reaction 3 all products from m = 2 to m = n − 1 are observed in significant amounts.

More recently, atomic transition metal ion chemistry in the gas phase has been pursued as a means of ionizing saturated polyolefins for molecular mass determination by MS analysis [13–15]. The lack of specificity in the reactivity of alkane C–C bond is one of several difficulties revealed in these studies. The reactions of the various atomic transition metal ions with the polyolefins fall under one of two categories. If the reactions are slow ($<<10^{-11}$ cm^3/molecule·s) relative to the experiment time frame, no product ions of interest are observed. Alternatively, if the reactions are fast, C–C bonds in the chain react without much selectivity and extensive chain fragmentation results. The presence of fragmentation products complicates quantitative measurement of simple hydrocarbon chains and will distort the MMD for saturated hydrocarbon polymers [14, 15].

More control of reaction selectivity may be achieved by using ligated-metal ion chemistry. For example, a recent study showed that while Fe^+, Co^+, and Ni^+ all react efficiently with alkanes, CpM^+ ions (Cp = η^5-cyclopentadienyl) react with ethane (producing $CpMC_2H_4^+$) only for M = Co and Ni [20]. The $CpFe^+$ ion is relatively unreactive [k_{Co}:k_{Ni}:k_{Fe} = 1.00:0.40:(<.01)] [20].

The $CpCo^+$ ion is of special interest. Not only is it the most reactive of the CpM^+ ions, but with small alkanes (n = 2–6) it reacts exclusively with C–H bonds and not

C–C bonds [20, 21]. Reaction products consist of $CpCo^{·+}$ bound to a hydrocarbon formed by eliminating hydrogen molecules from the reactant alkane. The carbon number of the reactant alkane is thus preserved in the ionized product. The reaction does not produce fragmentation of the alkane beyond dehydrogenation. Such a reaction might provide the basis for obtaining an accurate representation of the MMD for polyolefins. However, to date, no reactions of $CpCo^{·+}$ ion with n > 6 saturated aliphatic hydrocarbons have been reported.

In the present gas-phase study, we report results on the $CpCo^{·+}$ ion reactivity toward three medium chain length n-alkanes using Fourier-transform ion cyclotron resonance mass spectrometry (FT-ICR MS). Pentadecane (C-15), eicosane (C-20), and octacosane (C-28) serve as lower-molecular mass models of polyethylene. We find that the $CpCo^{·+}$ ion reacts predominantly by double H_2 loss from the CpCo-alkane ion complex for all three alkanes with no C–C bond cleavage observed. We observe an increase in reaction efficiency with increasing alkyl chain length. The results suggest that the $CpCo^{·+}$ ion is a promising cationization reagent for larger alkyl and polymeric systems.

Experiment

Samples

Cyclopentadienylcobalt dicarbonyl [$CpCo(CO)_2$], pentadecane (C-15), eicosane (C-20), and octacosane (C-28) were purchased from the Aldrich Chemical Company and used as received. [Certain commercial materials and equipment are identified in this paper in order to specify adequately the experimental procedure. In no case does such identification imply recommendation by the National Institute of Standards and Technology nor does it imply that the material or equipment identified is necessarily the best available for this purpose.]

Instrument/Measurements

All reaction rate measurements were carried out using a 3-tesla dual-cell Fourier transform ion cyclotron resonance mass spectrometer (Extrel FT/MS 2000) equipped with a heated multi-sample introductory system, described previously [22, 23]. Figure 1 shows a schematic of the FT-ICR MS system and dual cell. The $CpCo^{·+}$ ions were formed by 70-eV dissociative electron ionization of $CpCo(CO)_2$ leaked into cell 1. The neutral alkane was introduced into cell 2 by either a heated batch inlet or solids probe.

During the electron ionization event, ions are also formed from the alkane in cell 2 (Figure 1). To reduce complications from interfering reactions, ions generated from the neutral alkane were removed from cell 2 by applying −2 V potential to the trapping plate for 5 ms prior to ion transfer. The $CpCo^{·+}$ ions were transferred from cell 1 into cell 2 by grounding the conductance limit for approximately 240 μs (see Figure 1). After
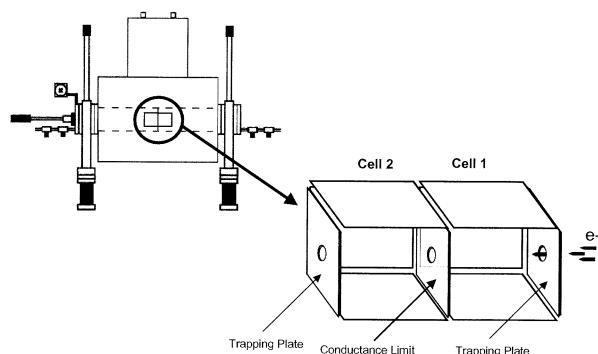
Figure 1. Schematic of 3-tesla Fourier-transform ion cyclotron resonance mass spectrometer is shown. Inset is a simple diagram of the dual cell.

transfer, the ions underwent a 1 s delay for radiative cooling [24]. This was to give ions and neutral molecules in the cell sufficient time to reach equilibrium with cell walls, which are at room temperature. The CpCo$^{\cdot+}$ ions were then allowed to react for a variable time (0.5 to 5 s) with the neutral alkane. The reactant and product ions were excited for detection using a broadband chirp [(11 to 2200) mass-to-charge range] [23a, c, 25]. Each time domain signal was recorded at a sampling rate of 5.3 MHz to yield a 132 k point transient that was multiplied by an apodization function and subjected to one zero fill prior to Fourier transformation [26]. After collection, residual ions were neutralized by applying a −10 V potential to the conductance limit and +10 V potential to the trapping plates for 5 ms. At least 15 acquisitions were summed for each mass spectrum used in the data analysis.

In order to account for reactions of ions other than the ion of interest, a background spectrum for each reaction time was also obtained. The background spectrum was acquired by ejecting the CpCo$^{\cdot+}$ ion (m/z 124) during the reaction delay. For example, Figure 2 shows (Figure 2a) the 750-ms reaction spectrum of CpCo$^{\cdot+}$ ion and pentadecane, (Figure 2b) the background reaction
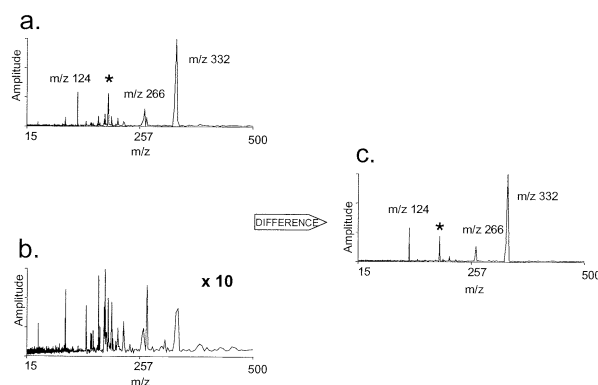

Figure 2. Mass spectra is given of (**a**) the 750-ms reaction of the CpCo$^{\cdot+}$ ion of m/z 124 with C-15 (MM 212 u), (**b**) background reaction, and (**c**) resultant reaction spectrum. The asterisk corresponds to a product formed between the CpCo$^{\cdot+}$ ion and the neutral precursor, Cp(CO)$_2$Co.

spectrum, and (Figure 2c) the resultant reaction spectrum.

Data Analysis

The reaction rate constants, reaction efficiencies, and product distribution were determined from FT-ICR MS data acquired for a series of reaction times. For all reactions studied, the neutral alkane concentration was much greater than the CpCo$^{\cdot+}$ ion concentration. Semi-logarithmic plots of the CpCo$^{\cdot+}$ ion decay show that the bimolecular reaction between the CpCo$^{\cdot+}$ ion and a given alkane follows pseudo first order kinetics in excess neutral alkane facilitating second order reaction rate constant determination for all three alkanes. The second order rate constants (k^{II}, cm^3/molecule·s) were derived from the neutral alkane concentration, determined from the nominal pressure (P_{alkane}, Pa), and the pseudo first order rate constant (k, s^{-1}), determined from the exponential CpCo$^{\cdot+}$ ion decay as a function of time (see eqs 1–3).

$$rate = k*[CpCo^{\cdot+}] \tag{1}$$

where

$$k\ (s^{-1}) = k^{II} * P_{alkane} \tag{2}$$

and

$$k^{II}\ (cm^3/molecule * s) = \frac{k}{P_{alkane} * 2.429 \times 10^{14}} \tag{3}$$

The reaction rate constants and product distributions presented are within a reproducibility of ±10%. However, the accuracy of the reaction rate constant is within ±50% due to the uncertainty in the pressure measurement. The alkane pressure is (P_{alkane}) is given by eq 4 which is based on a correlation method developed by Bartmess and Georgiadis [27].

$$P_{alkane} = P_{nitrogen} * \left[\frac{S_{alkane} * \alpha_{nitrogen}}{S_{nitrogen} * \alpha_{alkane}} \right] \tag{4}$$

A 70-eV electron ionization mass spectrum of the neutral alkane was acquired. A small amount of nitrogen gas was introduced into the cell, and a second 70-eV mass spectrum was collected. The nitrogen pressure reading ($P_{nitrogen}$) was corrected for the pressure difference between the cell and the hot cathode ionization gauge and assumed to reflect the actual nitrogen pressure in the cell. The alkane and nitrogen ion signal intensities (S_{alkane} and $S_{nitrogen}$, respectively) were determined from the second mass spectrum. $S_{nitrogen}$ value was corrected for the original background nitrogen in the cell. The nitrogen polarizability ($\alpha_{nitrogen}$) value was

used from an experimental measurement [28]. The polarizability of a given alkane (α_{alkane}) was estimated using the group polarizability method [28, 29].

In the gas phase, the upper limit to a bimolecular reaction is determined by the collision rate constant. In the present study, the gas-phase ion-neutral alkane collision rate constant (k_{coll}) depends largely on α_{alkane} and the reduced mass of the ion and neutral alkane (μ). k_{coll} was estimated using eq 5, where e is the elementary charge. Eq 5 is based on the Langevin theory of ion and neutral potential [30]. The size of the medium chain alkanes may raise the question on the collision rate approaching the hard-sphere limit. The estimates of the hard-sphere model give rates smaller than the collision capture model suggesting that the intermolecular forces still participate in the collision rate.
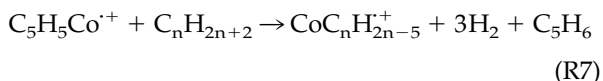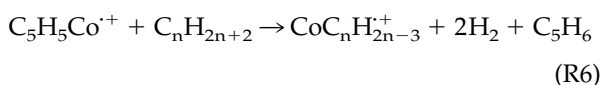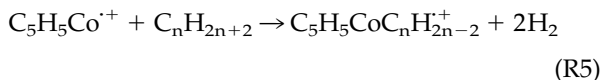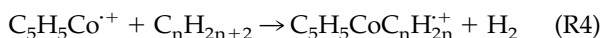
$$k_{coll} = 2\pi e \left(\frac{\alpha_{alkane}}{\mu} \right)^{1/2} \quad (5)$$

Because k_{coll} varies with the given alkane, k^{II} cannot be compared directly for a series of alkanes. The reaction efficiency, i.e., k^{II} divided by k_{coll}, normalizes the rate constants. One hundred percent reaction efficiency means that every collision between the reactant ion and neutral molecule results in a chemical reaction.

The product ion curves are parallel suggesting that ion products are all formed by primary reactions. The product distributions for the alkane reactions were determined from the ratio of the relative product ion abundances.

Results

Pentadecane (C-15), eicosane (C-20), and octacosane (C-28) were found to undergo the following reactions with the CpCo$^{\cdot+}$ ion (Reactions 4–7). The C$_5$H$_5$-designated moieties are likely Cp.

$$C_5H_5Co^{\cdot+} + C_nH_{2n+2} \rightarrow C_5H_5CoC_nH_{2n}^{\cdot+} + H_2 \quad (R4)$$

$$C_5H_5Co^{\cdot+} + C_nH_{2n+2} \rightarrow C_5H_5CoC_nH_{2n-2}^{\cdot+} + 2H_2 \quad (R5)$$

$$C_5H_5Co^{\cdot+} + C_nH_{2n+2} \rightarrow CoC_nH_{2n-3}^{\cdot+} + 2H_2 + C_5H_6 \quad (R6)$$

$$C_5H_5Co^{\cdot+} + C_nH_{2n+2} \rightarrow CoC_nH_{2n-5}^{\cdot+} + 3H_2 + C_5H_6 \quad (R7)$$

Reaction 4 corresponds to CpCo-alkane adduct ion minus two hydrogen atoms and is referred to in the present study as the single dehydrogenation (SD) pathway. Reaction 5 corresponds to nominal loss of two
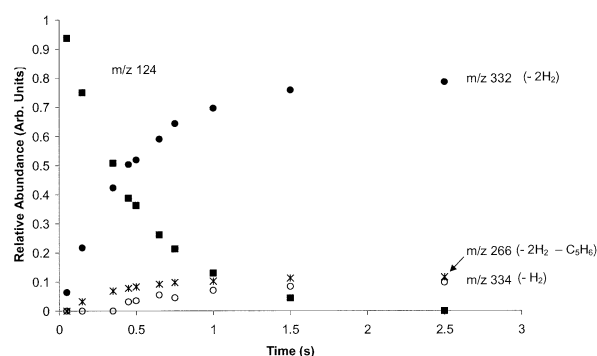

Figure 3. The plot of the kinetic data shows that the reaction of the CpCo$^{\cdot+}$ ion of m/z 124 (filled square) with C-15 (MM 212 u) produces ions of m/z 334 (open circle), m/z 332 (filled circle), and m/z 266 (asterisk).

hydrogen molecules from the adduct ion and is referred as the double dehydrogenation (DD) pathway. Reaction 6 corresponds to nominal loss of C$_5$H$_6$ from the DD product, and Reaction 7 corresponds to C$_5$H$_6$ and H$_2$ loss from the DD product. It is important to note that the DD pathway (Reaction 5) dominates the CpCo$^{\cdot+}$ ion reaction with all three alkanes. Its relevance to saturated hydrocarbon MS analysis will be discussed shortly.

Figure 3 shows a plot of the kinetic data for the reaction of CpCo$^{\cdot+}$ ion (m/z 124) and C-15 (MM 212 u). Relative abundances for ions of m/z 334, 332, and 226 correspond to the ions produced by Reactions 4–6, respectively. The DD production is the dominant pathway and accounts for approximately 80% of the product distribution (Table 1).

The CpCo$^{\cdot+}$ ion exhibits similar reactivity towards the C-20 and C-28 (Figures 4 and 5 and Table 1). CpCo$^{\cdot+}$ ion reacts with these alkanes predominantly by double dehydrogenation forming ion of m/z 402 for the reaction with C-20 (MM 282 u) and ion of m/z 514 for the reaction with C-28 (MM 394 u). Ions of m/z 404, 336, and 334 are three additional products observed for the reaction between the CpCo$^{\cdot+}$ ion and C-20 (Figure 4). The single dehydrogenated adduct corresponds to ion of m/z 404. Ions of m/z 336 and 334 correspond to nominal loss of 66 and 68 u from the DD product (Reactions 6 and 7, respectively). The neutral products are likely cyclopentadiene (CpH) and CpH/H$_2$. Products corresponding to CpH (m/z 448) loss and an additional H$_2$ loss (m/z 446) were also observed for the reaction between CpCo$^{\cdot+}$ ion with C-28 (Figure 5).

Table 1. Product distribution

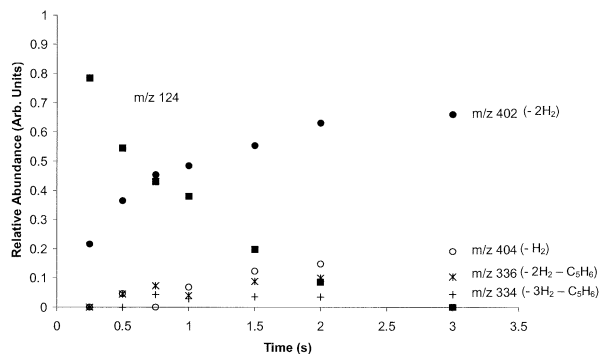| Alkane	$-2H_2$, %	$-H_2$, %	$-(2H_2 + C_5H_6)$, %	$-(3H_2 + C_5H_6)$, %
C-15	80	10	10	—
C-20	80	5	10	5
C-28	90	—	5	5

Figure 4. The plot of the kinetic data shows that the reaction of the CpCo$^{\cdot+}$ ion of m/z 124 (filled square) with C-20 (MM 282 u) produces ions of m/z 404 (open circle), m/z 402 (filled circle), m/z 336 (asterisk), and m/z 334 (plus sign).

Discussion

Single and Double Dehydrogenation

Dehydrogenation by the CpCo$^{\cdot+}$ ion has been classified an oxidative addition/reductive elimination reaction for small alkane systems [16, 21]. A similar type reaction likely occurs for the alkanes studied here. It is thought that the CpCo$^{\cdot+}$ ion preferentially attacks the C–H bond in the initial oxidative addition step due to the strong s character of metal-ligand antibonding orbital, i.e., LUMO (lowest unoccupied molecular orbital) [21]. It is interesting that the CpCo$^{\cdot+}$ ion reacts with n-alkanes exclusively by dehydrogenation, while the Co$^+$ ion reacts by dehydrogenation and dealkylation [15–17, 31]. It has been demonstrated by deuterium labeling, collision-activated dissociation, and ion-molecule studies that the apparent dehydrogenation reaction between Co$^+$ and n-butane goes by way of a C–C bond insertion [17, 31]. This result may explain, at least in part, the extensive fragmentation observed for the laser desorption MS analysis of the higher molecular mass alkane C-28 when Co$^+$ was used as the cationization reagent [15].

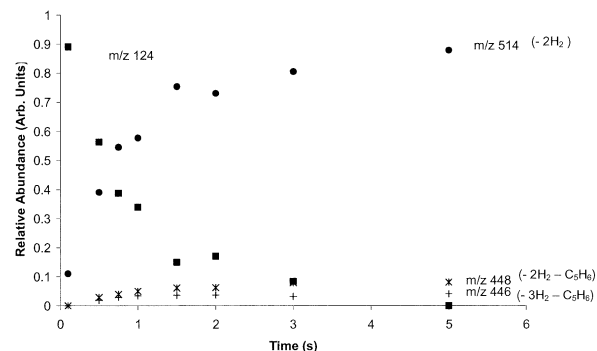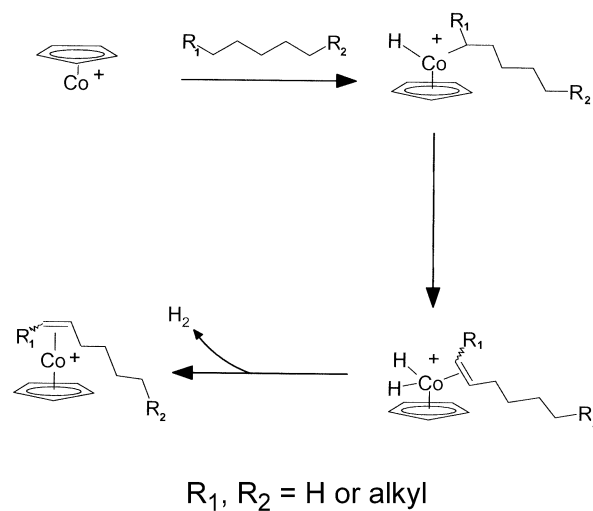Scheme **1** shows one possible mechanism for dehydrogenation of an alkane by the CpCo$^{\cdot+}$ ion. The
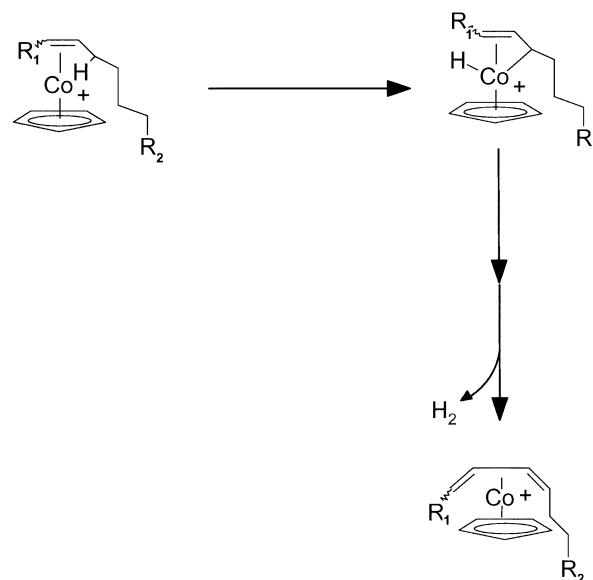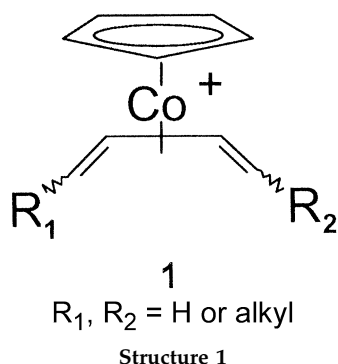

R_1, R_2 = H or alkyl

Scheme 1

CpCo$^{\cdot+}$ ion likely inserts into a secondary C–H bond, which is weaker than the primary C–H bond. A second hydrogen transfers to the Co, and the complex loses a hydrogen molecule. Re-insertion of Co into C–H bond of the allylic carbon followed by H atom transfer, and then H$_2$ loss leads formation of the double dehydrogenated product (for example, Scheme **2**).

Double dehydrogenation by the CpCo$^{\cdot+}$ ion is clearly the preferred reaction channel for C-15, C-20 and C-28 (Table 1). In a previous study, Jacobson and Freiser reported that double H$_2$ loss is twice as abundant in the CpCo$^{\cdot+}$ ion reactions with n-pentane and n-hexane as single H$_2$ loss [21]. Our results suggest that double H$_2$ loss dominates when a sufficient number of C–C sites are available.

Structure **1** is one plausible structure for the double

Figure 5. The plot of the kinetic data shows that the reaction of CpCo$^{\cdot+}$ ion of m/z 124 (filled square) with C-28 (MM 394 u) produces ions of m/z 514 (filled circle), m/z 448 (asterisk), and m/z 446 (plus sign).

R_1, R_2 = H or alkyl

Scheme 2

1

$R_1, R_2 = H$ or alkyl

Structure 1

$R_1, R_2 = H$ or alkyl

Scheme 4

dehydrogenated product. This 17-e⁻ product is similar to the strongly stabilized cobaltocenium ion (Cp_2Co^+) in that the pi orbitals of the Cp and butadiene-like ligand overlap strongly with Co d_{z^2} and p_z orbitals, stabilizing the metal complex.

C_5H_6 and C_5H_6/H_2 Loss

All three alkanes yield a small amount of product associated with Reactions 6 and 7, C_5H_6 and additional H_2 loss from DD product (Table 1). The formation of these products may result from excess internal energy in the ion-neutral molecule complex. Schemes **3** and **4** show possible mechanisms for Reactions 6 and 7, respectively. In Scheme **3**, an allylic H atom transfers directly to Cp ring forming CpH. Added stabilization of aromaticity drives the alkene to ring close forming a cyclopentadienyl type structure.

Collision-activated dissociation measurements on smaller alkane systems support the above rationale. In an earlier study, Jacobson and Freiser observed that collision activated dissociation measurements of the DD product for the CpCo-pentane and CpCo-hexane ion systems yielded a cobaltocenium-type product [21].
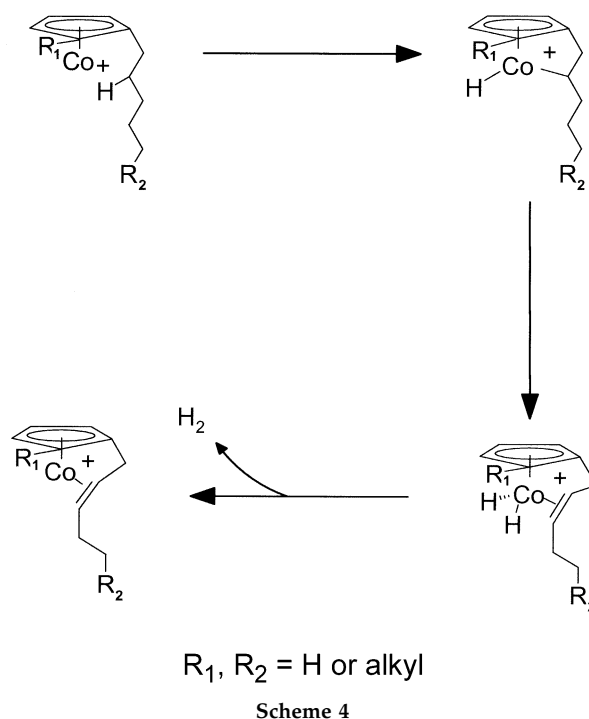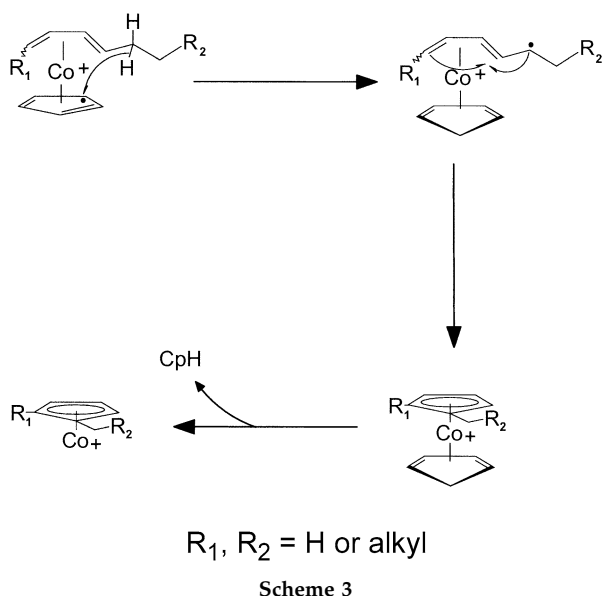
They proposed that upon H loss the alkene ring closes to form a cyclopentadienyl structure [21].

The FT-ICR MS experiments were carried out under low-pressure conditions [<10^{-5} Pa (10^{-7} torr)]. However, our future work with higher molecular mass hydrocarbon and polymer species will require the use of a matrix assisted desorption-ionization time-of-flight MS system. In these experiments, ionization will need to occur in a higher-pressure environment [>>10^{-5} Pa (10^{-7} torr)]. Deactivating collisions may stabilize the reaction complexes leading to the DD product (Reaction 5). Adduct formation often occurs in high-pressure gas-phase ion/molecule experiments [16]. Alternatively, activating collisions may lead to Reactions 6 and/or 7. Either way the most important requirement is that the predominant reaction pathway leads to a product characteristic of the original hydrocarbon. All products observed in the present study fulfill that requirement.

Reaction Efficiency and Chain Length

Table 2 gives the rate constants and efficiencies for the CpCo˙⁺ ion with C-15, C-20, and C-28. The reaction efficiency is defined as the percentage of collisions

$R_1, R_2 = H$ or alkyl

Scheme 3

Table 2. Rate constants and overall reaction efficiencies

Alkane	k_{exp}, ×10^{-10} cm³/ molecule·s	k_{coll}, ×10^{-10} cm³/ molecule·s	k_{exp}/k_{coll}, %
C-15	2.2	14	15
C-20	4.0	15	25
C-28	7.2	17	40

between the reactant ion and neutral molecule that lead to product. The overall reaction efficiency is 15% for C-15. The double dehydrogenation product is 80% of the total product yield. Therefore, twelve collisions in a hundred between the CpCo$^{\cdot+}$ ion and C-15 yields the double dehydrogenation product.

The reaction efficiencies given in Table 2 clearly show that the double dehydrogenation efficiency increases with increasing alkyl chain length. This relation is partially statistical in nature since the possible number of reactive C–C sites per molecule increase as the chain lengthens. We speculate that DD production may reach collision rate when the carbon chain length reaches ≈60 carbons. This suggests that formation of the DD product for hydrocarbons greater than 60 may be independent of chain length. This will be an important factor when studying longer chain length hydrocarbon and polyolefin systems.

The increase in reaction efficiency with chain length may also be attributed to the stabilization of ion/ molecule complex. Since the polarizability of the alkane increases with chain length, the complexation energy or stabilization energy increases for the ion/molecule complex as the alkyl chain length. This leads to longer lifetime of the complex and higher probability for the double dehydrogenation to occur. Interestingly, Milburn et al. noted that adduct formation between CpM$^+$ (M = second row alkali metals) and alkanes was found to depend on the size of the saturated hydrocarbon, increasing with increasing size until the collision rate is reached [32].

Conclusions

Results from this study on C-15 to C-28 suggest that the CpCo$^{\cdot+}$ ion may be a promising cationization reagent for saturated hydrocarbons larger than C-30. The CpCo$^{\cdot+}$ ion forms a double dehydrogenation product ion with all three n-alkanes studied that is characteristic of the original hydrocarbon. This double dehydrogenated product is the dominant species in all three reactions. The reaction appears to be a low-energy process since no C–C bond cleavage was observed under low-pressure conditions [<10^{-5} Pa (10^{-7} torr)]. Future work will include the use of the CpCo$^{\cdot+}$ ion to ionize higher molecular species analyzed using laser desorption time-of-flight mass spectrometry.

References

1. For a comprehensive discussion, see: Mountado, G.; Lattimer, R. P. *Mass Spectrometry of Polymers.* CRC Press: Boca Raton, 2002.
2. Hanton, S. D. *Chem. Rev.* **2001,** *101,* 527–569.
3. McEwen, C. N.; Peacock, P. M. *Anal. Chem.* **2002,** *74,* 2743–2748.
4. Lloyd, P. M.; Scrivener, E.; Malonay, D. R.; Haddleton, D. M.; Derrick, P. J. *Polym. Prep.* **1996,** *37,* 847.
5. Thomson, B.; Suddaby, K.; Rudin, A.; Lajoie, G. *Eur. Polym. J.* **1996,** *32,* 239.
6. Räder, H. J.; Schrepp, W. *Acta Polym.* **1998,** *49,* 272–293 and references therein.
7. Burlingame, A. L.; Boyd, R. K.; Gaskell, S. J. *Anal. Chem.* **1998,** *70,* 647R–716R and references therein.
8. Bauer, B. J.; Wallace, W. E.; Fanconi, B. M.; Guttman, C. M. *Polymer* **2001,** *42,* 9949.
9. Lin-Gibson, S.; Brunner, L.; Vanderhart, D. L.; Bauer, B. J.; Fanconi, B. M.; Guttman, C. M.; Wallace, W. E. *Macromolecules* in press.
10. Coessens, V.; Pintauer, T.; Matyjaszewski, K. *Prog. Polym. Sci.* **2001,** *26,* 337–377.
11. Matyjaszewski, K.; Coessens, V.; *Pure Appl. Chem.* **1999,** *A36(5&6),* 653–666.
12. Ji, H.; Sato, N.; Nakamura, Y.; Wan, Y.; Howell, A.; Thomas, Q. A.; Storey, R. F.; Nonidez, W. K.; Mays, J. W. *Macromolecules* **2002,** *35,* 1196–1199.
13. Kahr, M. S.; Wilkins, C. L. *J. Am. Soc. Mass Spectrom.* **1993,** *4,* 453–460.
14. Chen, R.; Yalcin, T.; Wallace, W. E.; Guttman, C. M.; Li, L. *J. Am. Soc. Mass Spectrom.* **2001,** *12,* 1186.
15. Chen, R.; Li, L. *J. Am. Soc. Mass Spectrom.* **2001,** *12,* 367–375.
16. Eller, K.; Schwarz, H. *Chem. Rev.* **1991,** *91,* 1121–1177 and references therein.
17. Armentrout, P. B.; Beauchamp, J. L. *Acc. Chem. Res.* **1989,** *22,* 315–321 and references therein.
18. Peake, D. A.; Gross, M. L.; Ridge, D. P. *J. Am. Chem. Soc.* **1984,** *106,* 4307–4316.
19. Peake, D. A.; Gross, M. L. *Anal. Chem.* **1985,** *57,* 115–120.
20. Ekeberg, D.; Uggerud, E.; Lin, H. Y.; Sohlberg, K.; Chen, H.; Ridge, D. P. *Organometallics* **1999,** *18,* 40–44.
21. Jacobson, D. B.; Freiser, B. S. *J. Am. Chem. Soc.* **1985,** *107,* 7399–7407.
22. Cody, R. B., Jr.; Kinsinger, J. A.; Ghadri, S.; Amster, I. J. *Anal. Chim. Acta* **1985,** *178,* 43–66.
23. For a review of FT-ICR MS, see: (a) Marshall, A. G.; Hendrickson, C. L.; Jackson, G. S. *Mass Spectrom. Rev.* **1998,** *17,* 1–35. (b) Amster, I. J. *J. Mass Spectrom.* **1996,** *10,* 1325–1337. (c) Dunbar, R. C.; Asamoto, B. *In FT-ICR/MS: Analytical Applications of Fourier Transform Ion Cyclotron Resonance Mass Spectrometry;* Asamoto, B., Ed.; VCH Publishers, Inc.: New York, 1991; pp 29–81.
24. Huang, F. S.; Dunbar, R. C. *J. Am. Chem. Soc.* **1989,** *111,* 6497–6500.
25. Marshall, A. G.; Verdun, F. R. *Fourier-Transforms in NMR, Optical, and Mass Spectrometry: User's Guide.* Elsevier: New York, 1990, Chap. 7.
26. Blackman, R. B.; Tukey, J. W. Particular Pairs of Windows. *In The Measurement of Power Spectra, from the Point of View of Communications Engineering.* Dover: New York, 1959; pp 98–99.
27. Bartmess, J. E.; Georgiadis, R. M. *Vacuum* **1982,** *33,* 149–153.
28. Miller, K. J. *J. Am. Chem. Soc.* **1990,** *112,* 8533–8542.
29. Vogel, A. *J. Chem. Soc.* **1948,** 1833.
30. Gioumousis, G.; Stevenson, D. P. *J. Chem. Phys.* **1958,** *29,* 294.
31. Jacobson, D. B.; Freiser, B. S. *J. Am. Chem. Soc.* **1983,** *105,* 5197–5206.
32. Milburn, R. K.; Frash, M. V.; Hopkinson, A. C.; Bohme, D. K. *J. Phys. Chem. A.* **2000,** *104,* 3926–3932.